ELSEVIER

Polymer 43 (2002) 279–288

polymer

www.elsevier.com/locate/polymer

Characterization of polyanhydride microsphere degradation by DSC

M. Sandor, N.A. Bailey, E. Mathiowitz*

Department of Molecular Pharmacology, Physiology and Biotechnology, Division of Biology and Medicine, Box G, Brown University, Providence, RI 02912, USA

Received 19 March 2001; received in revised form 24 August 2001; accepted 29 August 2001

Abstract

Microspheres (2.91 μm diameter) were formed from poly(fumaric-*co*-sebacic anhydride) (P(FASA)) using a phase inversion microencapsulation technique. Blank microspheres, protein-loaded microspheres, and raw polymer were degraded in water for varying lengths of time to determine how degradation affects morphology and crystallinity. The rate of degradation was subsequently characterized using differential scanning calorimetry (DSC) and step-scan alternating DSC (SSADSC). As evident by the changing melting peak ratios during degradation, the protein-loaded microspheres were found to degrade at a more rapid rate than both the blank microspheres and the raw polymer, respectively. This was most likely because the release of protein from the microsphere surface led to an increased surface area available for degradation of this surface-eroding polymer.

Keywords: Degradation; Microsphere; Differential scanning calorimetry

1. Introduction

Use of polymeric drug delivery systems offers many advantages over a single bolus administration of drug. Patient compliance, protection of the drug from highly acidic and potentially harmful environments of the body, e.g. the stomach, and sustained drug levels in the blood are all benefits of using polymers to deliver drugs. Polymeric drug delivery systems include rods [1–3], slabs [4,5], discs [6–8], films [9,10], and microspheres of various sizes [11,12].

Polymeric microspheres are drug delivery systems in the size range of 1 μm to about 2 mm. These spherical shaped devices are used to entrap small molecules, large proteins, and even DNA. The main purpose of these systems in our studies is protection during oral delivery to the human digestive tract or when injected under the skin, as in a depo formulation. In addition, these delivery systems are designed to enable controlled release of drug for a prolonged period of time. Microspheres are a useful type of delivery for systemic administration of drugs, since they can be used to encapsulate and protect a wide variety of drugs, and their small size can enable them to be injected intravenously and actually allow them to circulate in the bloodstream [13]. Additionally, delivery of sensitive drugs, such as plasmid DNA and proteins with short half-lives, can be conducted more efficiently by uptake of microspheres by target cells and subsequent release of therapeutic agent intracellularly [14].

Microspheres are fabricated by encapsulating a drug within a polymer matrix which is then released either by means of diffusion through the polymer matrix or degradation of the polymer when placed in a physiological environment [9]. Degradation, or hydrolytic cleavage of the polymeric backbone, begets one of the two types of erosion, bulk erosion or surface erosion, with the type based mostly on the hydrophilic/hydrophobic properties of the polymer and partly on the morphology of the system. Polymers which are relatively hydrophilic degrade by bulk erosion, allowing water to fully penetrate the polymer before beginning homogeneous degradation throughout the structure [15], whereas those that are relatively hydrophobic with extremely water-labile bonds degrade by surface erosion, breaking the bonds at the surface before allowing water to penetrate [16]. The morphology of a microsphere can play a significant role in the erosion mechanism by creating a very large surface area to volume ratio, which can actually make a surface-eroding polymer partially bulk eroding.

Polyanhydrides which are typically surface-eroding polymers, have been used to encapsulate and release a wide variety of drugs from polymeric systems of diverse morphologies [11,17–21]. Poly(fumaric-*co*-sebacic anhydride) (P(FASA)), the polymer we are examining in this

* Corresponding author. Tel.: +1-401-863-1358; fax: +1-401-863-1753.
E-mail address: edith_mathiowitz@brown.edu (E. Mathiowitz).

0032-3861/02/$ - see front matter
PII: S0032-3861(01)00612-7

paper, is a highly crystalline member of the polyanhydride family and has been used recently for delivery via the oral route because of its highly bioadhesive properties [19]. These properties allow for an increase in gastrointestinal transit time and consequential increase in the opportunity for drug to be delivered to the desired area. In addition, high sebacic acid content in copolymers has been shown to increase crystallinity [22].

When one develops a drug delivery system, one must focus on both the drug as well as polymer characterization. We have chosen to study a new method of encapsulation and analyze how morphology is affected during degradation of the system. We compare pure polymer, blank microspheres, and drug loaded microspheres. In this case, the drug is a protein, bovine serum albumin (BSA). Since addition of protein may alter the structure of the microsphere, it is important to study how it will affect microsphere degradation as well. Encapsulating a drug or protein may also lead to a change in the morphology. Therefore, it is important to characterize the degradation profiles of microspheres containing protein, compared to blank microspheres and the raw polymer. In this study, we will focus on characterization of polymer crystallinity by both conventional differential scanning calorimetry (DSC) and step-scan alternating DSC (SSADSC).

2. Materials and methods

2.1. Materials

Monomeric sebacic acid and fumaric acid were obtained from Sigma and copolymerized as previously reported to give P(FASA) [23].

Protein. The protein used to load microspheres, BSA, was obtained from Sigma.

HPLC grade dichloromethane was obtained from Allied Signal and analytical grade petroleum ether from Mallinckrodt.

2.2. Microsphere fabrication

Protein-loaded microspheres were made by a phase inversion technique [24]. Briefly, a 2% P(FASA) (20:80) (M_w 3212) polymer solution in dichloromethane (392 mg/19 ml) was mixed with a second solution of protein in water (8 mg/1 ml) at a ratio of 20:1. This two-phase system was probe sonicated on a Cole Parmer ultrasonic homogenizer at an amplitude setting of 20% for 30 s to form a fine water-in-oil emulsion of the two phases. This step is necessary to evenly disperse the protein within the polymer solution. Following sonication, the resulting emulsion was frozen in liquid nitrogen in order to stabilize it and prevent complete phase separation. The frozen emulsion was then lyophilized for 48 h to remove all water and solvent, leaving behind a solid product of protein particles entrapped within a polymer matrix. The dried product (400 mg) was then resuspended in dichloromethane (20 ml), producing a suspension of insoluble protein particles in solubilized polymer (2% solution). This suspension was then quickly introduced into a non-solvent bath of petroleum ether at a solvent:non-solvent ratio of 1:50. Upon contact with the non-solvent, the polymer spontaneously precipitated from solution, forming spherical polymeric particles encapsulating the protein. These resulting microspheres, which were theoretically loaded with 2% BSA protein (w/w), were then collected with a high pressure filtering system. Unloaded microspheres containing no protein were also fabricated as a control using the same method in order to impart the same thermal history. Microsphere particle size was found to have a median diameter of 2.91 μm by laser light scattering techniques. Additional aliquots of raw polymer were pulverized into a fine powder and also tested.

2.3. Microsphere degradation

Blank microsphere, protein-loaded microsphere, and bulk polymer aliquots of 10–20 mg were placed in microcentrifuge or 15 ml conical tubes and allowed to degrade at 37°C in HPLC-grade water at a concentration of 10 mg/ml for various amounts of time: 1, 4, 8, 24, 48, and 72 h, and 1 and 4 weeks. At each timepoint, the tubes were centrifuged, the supernatant was removed and discarded, and the remaining pellet was frozen and lyophilized. Prior to lyophilization of each sample, the water was changed several times at regular intervals. This step removed water soluble low molecular weight degraded species from the remaining insoluble polymer samples. These additional changes aided in maintenance of a neutral pH which helped to prevent acid-catalyzed degradation of the polymer which would otherwise contribute a further variable to affect the degradation rate [25].

2.4. Differential scanning calorimetry

Dried P(FASA) pellets were used to determine the changing thermal properties of the degrading microspheres and bulk polymer. Samples were analyzed on a Perkin–Elmer Model DSC-7 differential scanning calorimeter. The DSC was calibrated for temperature and enthalpy using the melt of indium ($\Delta H = 28.4$ J/g). Samples (5.00 ± 0.2 mg) were contained in an aluminum pan with lid, and an empty pan with lid was used as a reference. A baseline subtraction was made to correct for any slope or variation in heat transfer effects by heating the DSC with an empty pan in both the sample and reference holders under identical conditions as in the experiment and then subtracting the resultant curve. Polymer was analyzed to determine the effects of degradation and thermal history imparted to it during fabrication. Samples were heated from −20 to 200°C at 10°C/min, using nitrogen as a purge gas at 20 ml/min. Thermograms (traces) were analyzed to determine the melting point (T_m) and the enthalpy of melting (ΔH_m) of the samples. Percentage of total enthalpy of each observed melting peak was calculated

and attributed to crystalline species assumed to be present in the sample.

2.5. Step-scan alternating DSC

SSADSC measurements were performed on a Perkin–Elmer Pyris 1 DSC, using the SSADSC software provided. Samples prepared in the same manner as for conventional DSC were heated at various rates and held for various isothermal periods to determine the conditions that gave the best resolution of the deconvoluted curves. Heating rates varied between 1.0 and 5.0°C/min for the overall heating rate over the range of 0–130°C. Helium was used as a purge gas at 20 ml/min. A baseline subtraction was made to correct for any slope or variation in heat transfer effects by heating the DSC with an empty pan in both the sample and reference holders under identical conditions as in the experiment and then subtracting the resultant curve. The data was subsequently analyzed to determine the reversing and non-reversing components.

2.6. Fourier transform infrared spectroscopy (FTIR)

Degraded and undegraded samples were analyzed on a Perkin–Elmer model 1725 × FTIR. Samples were ground with a mortar and pestle and mixed with KBr at a ratio of 1:100. The mixture was then pressed into a pellet and spectra analyzed from 400 to 4000 cm^{-1}. The anhydride (1807.12 cm^{-1}) and acid (1701.91 cm^{-1}) peaks were measured and their relative areas compared in order to determine the composition of the remaining sample.

3. Results and discussion

3.1. Differential scanning calorimetry

Microspheres with a mean diameter of 2.91 μm were made by a phase inversion technique during which the polymer spontaneously precipitated from solution upon contact with a non-solvent. Encapsulation of protein during this process produced microspheres with a matrix type morphology in which the 2% loaded protein was homogeneously dispersed.

P(FASA) protein-loaded microsphere samples exhibited interesting thermal transition patterns following degradation. Initially, a bimodal melting peak was observed with the primary melting peak of greater magnitude than the secondary melting peak. Over time, the relative magnitude of the primary melting peak decreased and the secondary melting peak increased. A tertiary melting peak also developed which was assumed to be a result of oligomers forming due to degradation (for example see Fig. 1 over the time period of 1 week). We speculate that this melting peak is due to oligomers since low molecular weight pre-polymers were shown previously to melt at 67 and 79°C (for sebacic acid and fumaric acid prepolymer respectively), while

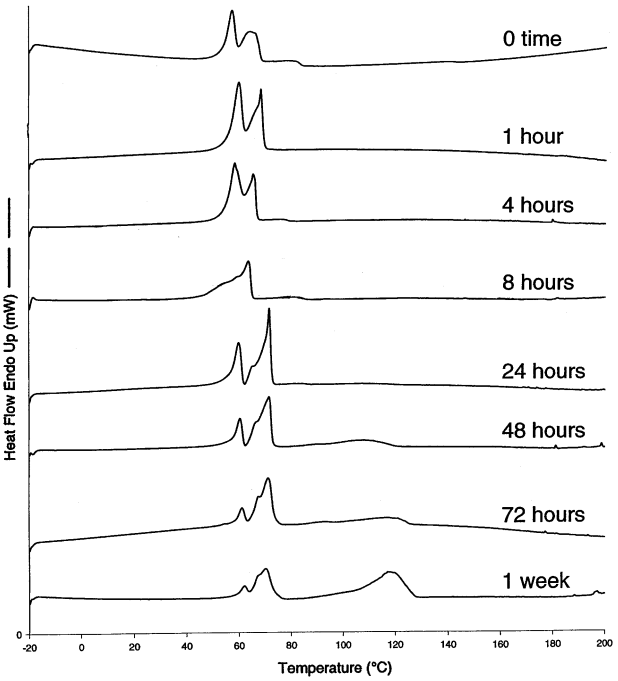

Fig. 1. DSC thermograms of P(FASA) microspheres loaded with protein (2% loading) up to a degradation time of 1 week.

sebacic acid monomer melted at 136°C. Fumaric acid monomer sublimes at approximately 200°C. Smaller, less prominent peaks that appear on some of the thermograms (traces) between 73 and 110°C are also assumed to be smaller polymeric or oligomeric fragments due to degradation but are not analyzed or included in the overall enthalpy of melting. Additional evidence for the identification of the tertiary peak comes from the data obtained via FTIR. For samples analyzed from time zero to 1 week degradation, it is evident that the acid peak (1701.91 cm^{-1}) is becoming larger, relative to the anhydride peak (1807.12 cm^{-1}) as degradation time progresses (An example is shown for protein-loaded microspheres in Fig. 2 and Table 1). Initially, the undegraded sample contained 2.6% acid species which increased to 37.6% by 8 h. After this point, the acid content continued to increase linearly, at a rate of about 7.2% per

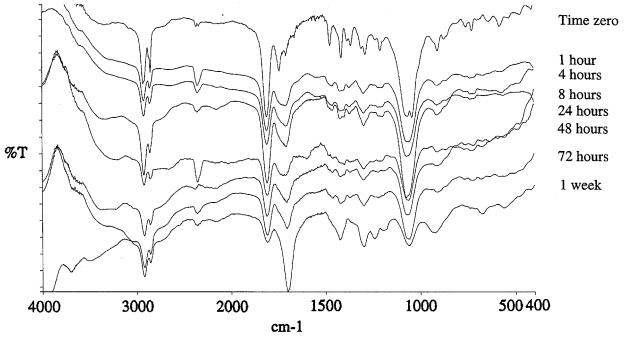

Fig. 2. FTIR scans of protein-loaded P(FASA) microspheres degraded over time.

Table 1
Correlation between degradation time and relative peak areas for anhydride and acid species in protein-loaded microspheres analyzed by FTIR

Degradation time	Percentage anhydride (%)	Percentage acid (%)
0 h	97.4	2.6
1 h	60.6	39.4
4 h	56.6	43.4
8 h	62.4	37.6
24 h	59.0	41.0
48 h	54.0	46.0
72 h	49.3	50.7
1 week	15.1	84.9

day, reaching a maximum of 84.9% by 1 week. Since the anhydride bonds of P(FASA) are extremely water-labile, they are broken during degradation, and each creates two acid end groups. The presence of this relatively increasing acid peak, then, gives evidence that as degradation is occurring, anhydride bonds are breaking, and more and more shorter chain oligomers are retained within the sample. It is believed that these shorter chain oligomers are the species which gives rise to the tertiary melting peak. Additionally, these acidic oligomeric species have been found to melt at higher temperatures than those of their pre-polymer counterparts [26] which would explain why they melt in the range of 73– ~ 115°C.

On closer examination of the DSC thermograms (traces) for protein loaded microspheres, the total change in enthalpy upon melting remained fairly constant for each of the degradation timepoints, even though the relative percent of total enthalpy for each peak varied (see Table 2). This constant enthalpy was maintained by a significant decrease over time of the primary melting peak (attributed to smaller crystals), a fairly constant enthalpy for the secondary melting peak (attributed to the melting of large crystals), and a significant increase over time in the melting of oligomers (the tertiary melting peak).

The degradation behavior of protein-loaded microspheres was compared to both unloaded control microspheres and raw polymer. When undegraded samples were initially heated, the raw polymer showed a single endotherm with an enthalpy of melting of 110.4 J/g and a T_g with a ΔC_p of 0.35 J/g at 32.9°C, control microspheres showed a single endotherm with a low temperature shoulder of total enthalpy

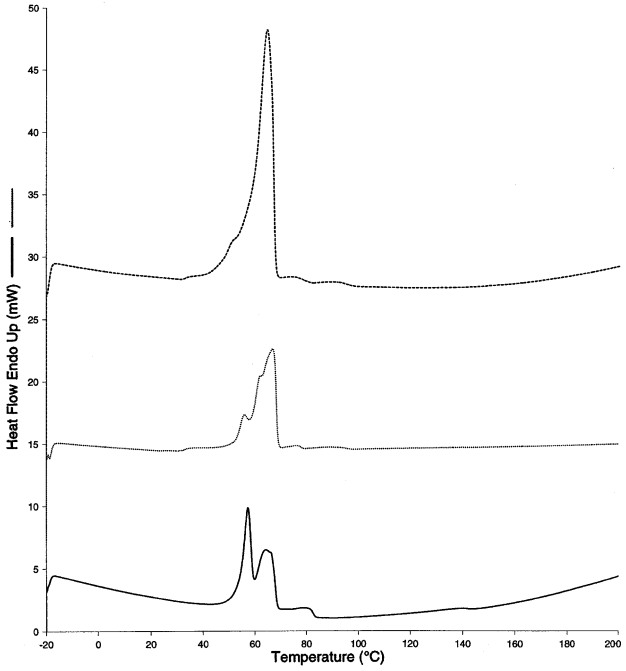

Fig. 3. Comparison between DSC thermograms for raw polymer (dashed line), control microspheres (dotted line), and protein loaded microspheres (solid line) at time zero.

98.8 J/g and a T_g with a ΔC_p of 0.15 J/g at 32.9°C, and protein-loaded microspheres displayed two distinct endotherms with total enthalpy change on melting of 99.1 J/g (±0.2) and no detectable T_g. (see Fig. 3). The enthalpy of melting values for both the control and protein loaded microspheres were within experimental error of each other, indicating that protein probably does not interfere with the crystalline structure of the undegraded microspheres. The enthalpy of melting for both types of microspheres was shown to be smaller than that of the raw polymer. The only difference in the treatment of these materials that might account for the variation in thermal history was the rapid precipitation into a non-solvent experienced by the microspheres during fabrication in contrast to the slow cooling to room temperature followed by polymerization of the raw polymer.

With the commencement of degradation, the enthalpies of melting of all the samples increased significantly initially

Table 2
Correlation between degradation time and enthalpy for protein loaded microspheres; partial and total enthalpy

Degradation time	Primary melt (J/g)	Secondary melt (J/g)	Tertiary melt (J/g)	Total enthalpy (J/g)
0 h	51.6	47.4	–	99.1
1 h	68.0	56.5	–	124.6
4 h	83.6	47.3	–	131.0
8 h	49.4	47.7	–	97.1
24 h	39.5	72.5	–	112.0
48 h	22.2	66.7	37.6	126.5
72 h	9.5	66.7	42.3	118.5
1 week	3.8	33.7	95.7	133.2

but remained fairly constant between 1 h and 1 week degradation, averaging 120.4 ± 12.6 J/g for the protein loaded microspheres, 121.6 ± 14.5 J/g for the control microspheres and 131.7 ± 8.0 J/g for the raw polymer. The increases in the enthalpy of fusion are attributed to the loss of amorphous surface material in both the control microspheres and the polymer, thus relatively decreasing the amorphous fraction and increasing the crystalline fraction of the sample. The preferential loss of amorphous material has been previously reported [27] and is evident by the decrease in ΔC_p at 39°C from 0.352 J/g for raw polymer and 0.145 J/g for control microspheres, respectively, to negligible values by 1 h of degradation.

Differences in these overall enthalpies led to a closer examination of individual enthalpies and melting temperatures following various intervals of hydrolytic degradation.

Fresh undegraded protein-loaded microspheres exhibited a bimodal melting peak (inclusive of a primary and a secondary melting peak) at 57.4 and 66.2°C. After 1 h of exposure to water, the melting points shifted to 60.0 and 68.5°C, and showed a corresponding increase in enthalpy from 99.1 to 124.6 J/g. The 8 h timepoint yielded a primary melting peak with an enthalpy (49.4 J/g) that was significantly lower than that of the previous primary melting peaks. The overall enthalpy of the sample at this point was also reduced to 97.1 J/g. Although this melting trace appeared similar to one broad melting peak (see Fig. 1), its appearance was actually due to the simultaneous decreasing of the primary peak and increasing of the secondary peak at similar rates. This type of behavior was also observed for microspheres loaded with other proteins, such as alcohol dehydrogenase and thyroglobulin (data not shown).

The overall enthalpy of protein loaded microspheres increased again to 112.4 J/g at 24 h as both melting points also increased significantly (60.0 and 71.78°C) and remained elevated without further significant changes in melt temperature for the remainder of the experiment (4 weeks).

It was also at this 24 h timepoint that the bimodal melting peak, which before had been viewed as two overlapping peaks, was resolved into two completely distinct peaks with a small shoulder (65.4°C) developing on the beginning of the secondary melting peak. At this point, the relative sizes of the two enthalpies had also been transposed, with the secondary melting peak increasing in size relative to the primary melting peak. Although P(FASA) degrades mainly by surface erosion, the size of the microspheres might actually contribute to an erosion profile that is partly surface-erosion and partly bulk-erosion. The spaces left by degraded amorphous material might enable water to further enter the structure to begin erosion of small crystals, which are more susceptible to degradation than large crystals as a result of higher surface energy. Leaching of protein from the protein loaded microspheres most likely contributed to even further destabilization of their crystalline structure since by 8 h of exposure to water, 53.6% of the loaded protein had been released (data not shown), leaving large pores on the surface of the microsphere, and both the T_m of the primary species and its enthalpy of melting decreased.

Loss of small crystals leads to a relative increase in the number of large crystals per unit mass, and therefore the enthalpy of the primary melting peak would decrease as the secondary melting peak increases. Alternatively, the lower molecular weight species that are forming due to degradation may have more mobility which would allow for a more rapid partial melting. These shorter chains would then be free to contribute to the formation of a more perfect crystal and, therefore, the size of the second melting peak would grow in size relative to the first melting peak.

At 48 h, a smaller, broader melting peak also began to appear at higher temperatures on the thermograms (traces) of the protein-loaded microspheres (see Fig. 1). Some of the polymer has been reduced to insoluble oligomers which can be seen to melt at higher temperatures on the thermogram (trace). The formation of these oligomers maintains the total enthalpy of the sample, although a smaller proportion is now from the polymer itself. By 4 weeks, the melting peak appeared as a single broad peak, with a melting temperature very similar to that of the secondary melting peak of the polymer.

The degradation thermograms (traces) were then analyzed for the raw polymer and control microspheres and compared to those for the protein loaded microspheres (see Tables 3 and 4 for the changes in enthalpy of the control microspheres and raw polymer, respectively).

Thermogram (trace) changes for control microspheres were similar to that of protein-loaded microspheres, with the inception of a bimodal melting peak (55.6 and 67.0°C) that became more distinct after 1 h degradation. From 1 to

Table 3
Correlation between degradation time and enthalpy for control microspheres; partial and total enthalpy

Degradation time	Primary melt (J/g)	Secondary melt (J/g)	Tertiary melt (J/g)	Total enthalpy (J/g)
0 h	16.3	80.4	2.1	98.8
1 h	84.3	47.9	–	132.2
4 h	92.7	29.1	4.2	126.0
8 h	114.3	10.2	0.3	124.8
24 h	39.2	79.8	5.1	124.1
48 h	24.5	72.1	36.0	132.6
72 h	17.9	69.4	2.8	90.1
1 week	7.0	50.8	63.5	121.3

Table 4
Correlation between degradation time and enthalpy for raw polymer; partial and total enthalpy

Degradation time	Primary melt (J/g)	Secondary melt (J/g)	Tertiary melt (J/g)	Total enthalpy (J/g)
0 h	109.1	–	1.3	110.4
1 h	122.6	–	0.5	123.1
4 h	119.2	–	11.6	130.8
8 h	121.4	–	7.5	128.9
24 h	101.8	26.8	3.1	131.7
48 h	82.6	30.5	15.0	128.1
72 h	69.1	39.9	21.4	130.4
1 week	64.3	28.4	56.0	148.7

8 h, the change in enthalpy of the secondary melting peak decreased relative to the first. At 24 h, just as in the protein-loaded microspheres, two distinct peaks became evident (60.4 and 70.9°C). These two peaks were evident through 1 week of degradation.

Although control microspheres, for the most part, behaved very similarly to those loaded with protein, a difference was seen at 4 and 8 h degradation. Control microspheres have a sharp reduction in the endotherm at 4 h exposure to water (Table 3), whereas a reduction does not occur for the protein-loaded microspheres until 8 h (Table 2). This gives evidence that the protein was aiding in the maintenance of the polymer crystal structure. Large amounts of protein (particle size 5–150 nm by TEM) are entrapped within the polymer near the surface of the microsphere (approximately 1–3 μm in diameter), allowing less space to be taken up by amorphous material. Once protein has escaped from the surface of the microspheres, the overall surface area is increased, creating an opportunity for water to further penetrate the microspheres and degrade the smaller crystals. The infiltration of water into the structure of the microspheres is even greater than that allowed by the loss of amorphous material in the control microspheres and alters the degradation profile by creating an even larger surface area than that of the control microspheres. This leads to an increased degradation rate, which is evident by the increase in the percentage of the enthalpy due to the tertiary melting peak for protein-loaded microspheres as compared to that of the control microspheres (Fig. 4). Additionally, a small baseline transition resembling a T_g at 32.9°C is evident for fresh control microspheres that is not present for the protein-loaded microspheres, indicating that the control microspheres have a higher amorphous content.

In contrast, P(FASA) raw polymer did not exhibit thermograms similar to those of the control or protein-loaded microspheres. The fresh raw polymer yielded a single melting peak at 64.7°C with a small shoulder at 51.9°C which could no longer be identified by 4 h degradation. This single melting peak corresponded well with the primary melting peak seen in the protein-loaded microspheres. A bimodal melting peak began to materialize at 24 h degradation (64.8 and 70.4°C) and was evident through 1 week, but never separated into two distinct peaks as seen in the control and protein-loaded microsphere samples. The primary melting point of each bimodal melting peak corresponded to the single melting peak that existed earlier in the degradation. This data indicates that processing of the polymer to produce microspheres enables larger crystals to form, since only microspheres, and not raw polymer itself, yielded a more perfect, larger crystal as shown in the secondary melting peak. The solubilization of the polymer in dichloromethane during microencapsulation allows the chains to move freely which then immediately precipitate/crystallize upon contact with the non-solvent. It is also possible, however, that the microspheres which are smaller than the pulverized raw polymer particulate will degrade more quickly, given their higher surface area to volume ratio. The materialization of the secondary crystalline species might be partially due to the speed of degradation.

3.2. Step-scan alternating DSC

SSADSC is a recently commercialized technique in

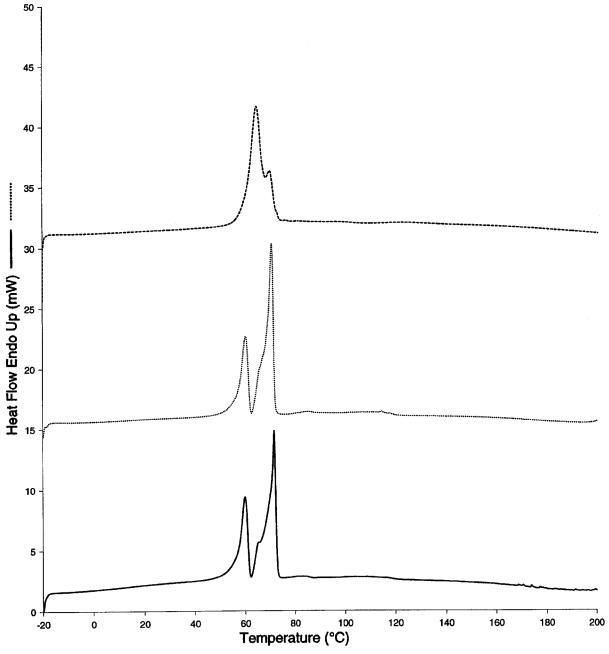

Fig. 4. Comparison between DSC thermograms for raw polymer (dashed line), control microspheres (dotted line), and protein loaded microspheres (solid line) degraded for 24 h.

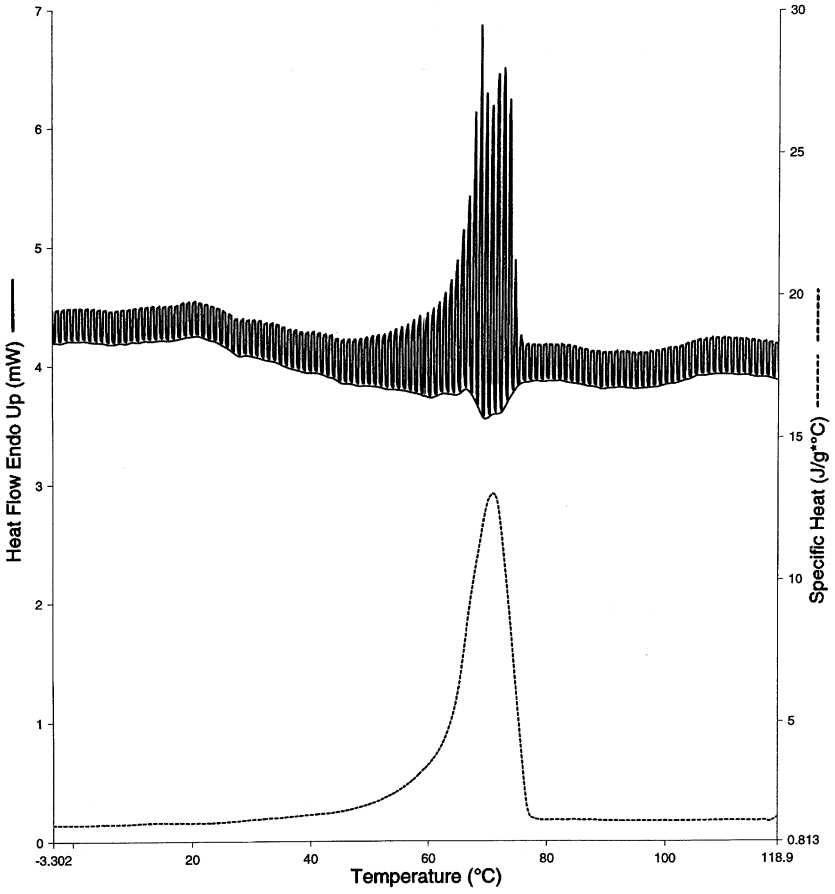

Fig. 5. Modulated heat flow (solid line) and reversing (dashed line) components of SSADSC thermogram of P(FASA) control microspheres at time zero.

which the sample follows a heat-hold temperature program to obtain additional information about the samples properties. By conventional DSC, the resolution of the trace can be improved by using a slower heating rate or smaller sample, resulting in a loss in sensitivity, as the signal-to-noise ratio decreases and the limit of the instrument is approached. The only way to improve sensitivity is by increasing the heating rate or sample mass, resulting in a loss in resolution. The complexity of this issue led to the development of modulated temperature DSC (MTDSC) and later SSADSC. In MTDSC, a heat–cool temperature profile, generally sinusoidal, is superimposed on the linear heating rate of the DSC. The addition of the sinusoidal signal results in a constantly varying heating rate and allows the type of complex analysis which would only be possible in conventional DSC by doing multiple experiments at various heating rates. The modulated temperature and resultant modulated heat flow can be deconvoluted using a Fourier transform to give reversing and non-reversing components, allowing separation of overlapping transitions. SSADSC is a more simplified approach since there is no complex Fourier transform involved in data deconvolution and is similar to the approach outlined by Reading [28] since it does not involve a phase lag and because the data is separated into reversing and non-reversing components rather than in-phase and out-of-phase.

The equation to describe heat flow is derived from a simple equation based on thermodynamic theory in which

$$\mathrm{d}H/\mathrm{d}t = C_\mathrm{p}(\mathrm{d}T/\mathrm{d}t) + f(T,t) \quad (1)$$

where $\mathrm{d}H/\mathrm{d}t$ is the heat flow, C_p is the reversible part (heat capacity term) and $f(T,t)$ is the kinetic or non-reversing term (isothermal) and is a function of time and temperature [29,30]. Therefore, the heat capacity on heating is simply related to the change in heat flow divided by the change in temperature:

$$C_\mathrm{p} = (\mathrm{d}H/\mathrm{d}t)/(\mathrm{d}T/\mathrm{d}t) \quad (2)$$

The non-reversing heat flow is, therefore, simply the change in heat flow that occurs during the isothermal segment of the heat-hold experiment. The total heat flow is taken to be the average of the heat flow response to the heat-hold temperature program. In this way, the total heat flow can be separated into the reversing and non-reversing components, because the reversing component is only observed on the heating part of the cycle and the non-reversing only on the isothermal. Since both the heat capacity equilibration and DSC equilibration are rapid, the C_p

calculation is said to be independent of kinetic processes [30]. This differs from MTDSC as there is no Fourier transformation for deconvolution of the traces and no phase lag component to the analysis [29,31,32]. The term non-reversing indicates that at the time and temperature of the measurement, the process was not reversing even though it may have been reversible (e.g. crystallization). Similarly at the glass transition, the reversing signal does not include all the enthalpy that is reversible because it is time dependent. Rather, it comprises only the part that is reversing at that modulation frequency. Therefore, the term reversing is chosen over reversible and non-reversing over irreversible [31]. Reported advantages of MTDSC over conventional DSC include improved sensitivity and resolution [29,33], separation of overlapping reversing and non-reversing transitions [34] and more accurate heat capacity values [35]. SSADSC is said to further offer advantages over MTDSC in that as previously stated there is no complex Fourier transform involved, there is no curve subtraction as the irreversible (non-reversing) response is directly extracted from the isothermal response, and it is three times faster than MTDSC. As the main application of SSADSC is enhanced characterization of the T_g, it was used to try to determine the glass transition of the degraded samples, not detectable by conventional DSC, and improve the resolution of the melting peaks.

Variation in sample analysis parameters was initially investigated to determine the parameters that gave the best overall resolution for raw polymer, control microspheres, and protein loaded microspheres which have been degraded in water for 24 h. This included heating at 10.0, 5.0 and 2.0°C and holding for 0.5 min in all cases. The heat flow response to the step scan temperature measurements was recorded and the data subsequently analyzed to determine the reversing and non-reversing components (see Fig. 5). The reversing trace showed clearly defined peaks with improved resolution compared to those by conventional DSC. As expected, the slower overall heating rate gave the best resolved peaks (see Fig. 6, for reversing components at an overall heating rate of 5.0, 1.0 and 0.5°C/min). SSADSC enabled improved resolution at slower heating rates whilst maintaining the sensitivity of the instrument (in conventional DSC, at slower heating rates the signal-to-noise ratio decreases, obscuring the trace). Despite the improved sensitivity, no glass transition could be detected on the degraded samples. This may mean that there is no amorphous material left in the sample and that it degraded rapidly as indicated by the conventional DSC results.

A study of the melting traces agreed with those obtained by conventional DSC, with the protein loaded microspheres degrading at a faster rate than either the blank microspheres or the polymer, respectively (see Fig. 7). The degraded protein loaded microspheres produced a single peak corresponding to the secondary melting peak observed with conventional DSC, indicating that smaller crystals (assumed to melt at a lower temperature, the primary

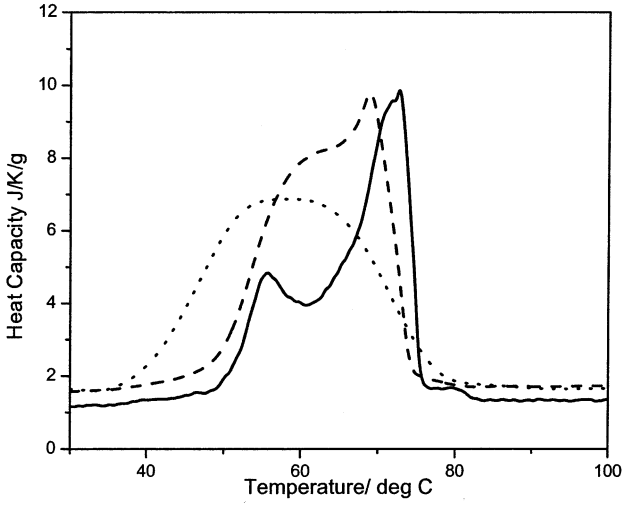

Fig. 6. SSADSC reversing components of undegraded P(FASA) control microspheres when heated at an overall heating rate of 0.5°C/min (solid line), 1.0°C/min (dashed line), and 5.0°C/min (dotted line).

melting peak) were degraded more readily than larger crystals. It was also assumed that they degraded more rapidly than control microspheres because protein leached from the microspheres, leaving a larger surface area for degradation to occur. Slight variations in degradation time may explain why a single peak is observed by SSADSC whereas a bimodal peak was observed by conventional methods. A more pertinent question is why this did not occur for the control microspheres. These microspheres produced peaks corresponding to the melting of both small and large crystals, but not oligomer. This can possibly be attributed to the slower degradation of control microspheres as opposed to protein loaded microspheres which have no remaining small crystals at this point. Alternatively, it may be a result of melt and recrystallization as a result of the heat-hold temperature program producing more perfect crystals. This may occur preferentially in the protein loaded spheres as there is more freedom for the polymer chains in the bulk material to reorganize due to the higher surface area. However, a further study is needed to confirm this. There was some evidence of the melt-recrystallization process occurring on heating observed as an exothermic peak in the non-reversing component as it passes through the melt. As both the reversing and non-reversing components contain elements of endothermic melting, the proportion of the melt that is reversing is relative to the other experimental conditions and is not a finite value [36]. Many of the problems in analyzing modulated data in this region are due to the factors effecting relative contributions of the reversing and non-reversing components and much research considers the validity of analysis in this region.

Endotherms were observed in the degraded raw polymer at temperatures corresponding to the melting of both small and large crystals, as well as that of oligomer [27]. It was proposed that the small size of the degrading particles might

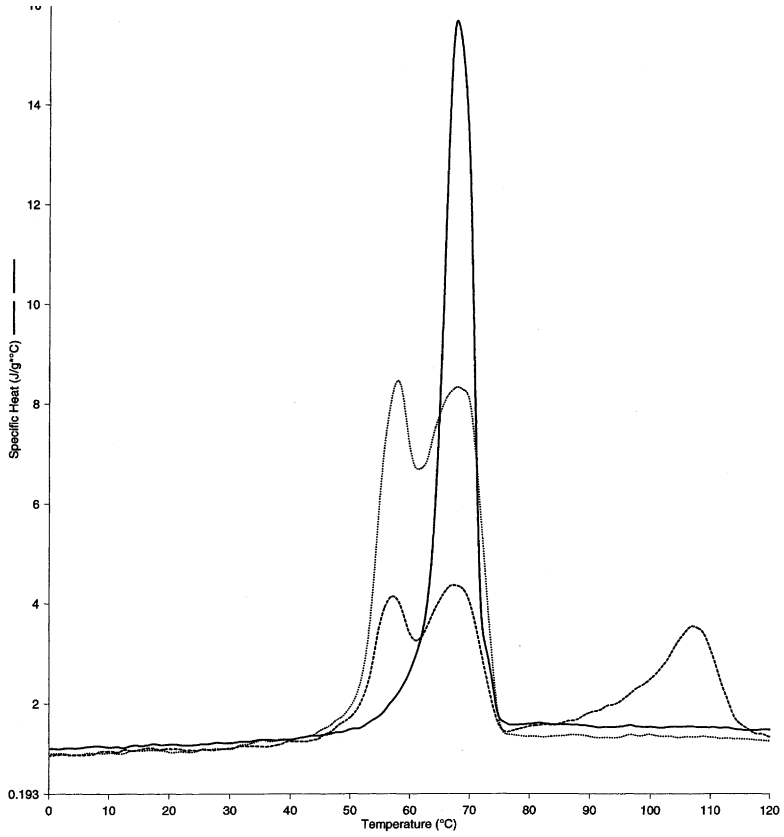

Fig. 7. SSADSC reversing components of P(FASA) raw polymer (dashed line), control microspheres (dotted line), and protein loaded microspheres (solid line) degraded for 24 h.

contribute to partial bulk erosion which would lead to some degradation and formation of oligomer within the microsphere as well as the expected degradation on the particle surface. In the microspheres which have a larger surface area to volume ratio, any oligomer formed within can easily diffuse into the buffer. However, in the raw polymer whose particles have a smaller surface area to volume ratio, oligomers have to diffuse further through the sample and may become trapped within, yielding an evident melting peak.

The non-reversing trace gave little additional information but this may be as a result of the small sample size used (1–2 mg) and so a more detailed study should be carried out using a larger sample size and increased number of degradation time points. Previous work by MTDSC has shown that the results obtained for melting traces by this technique should be treated with caution as the proportion of the reversing to non-reversing peak varies with experimental parameters, e.g. the non-reversing peak increases with increasing heating rate [37].

4. Conclusions

The degradation rates of control and protein loaded microspheres were compared to that of raw polymer to determine whether the microsphere fabrication process or protein loading has a significant effect. The rate of degradation was studied quantitatively using DSC and SSADSC.

Both protein loaded and control microspheres had a higher initial amorphous content than the pulverized raw polymer, most likely due to the spontaneous precipitation/crystallization involved in the microencapsulation process. The melting endotherm of P(FASA) microspheres was shown to be unaffected by protein loading, indicating that this process does not interfere with the crystallization behavior on formation of microspheres. However, microspheres loaded 2% with protein degraded at a faster rate as shown by the more rapid loss of amorphous material compared to blank microspheres. This was due to protein diffusion from the microsphere surface, leaving behind an increased surface area and enabling more rapid penetration by water which begets more rapid degradation. Because of their small size, P(FASA) microspheres seemed to exhibit traits indicative of bulk erosion in addition to the expected surface erosion profile.

SSADSC gave better resolved peaks than conventional DSC as a result of the slower overall heating rates. However, further investigation of the effect of the modulation parameters on the relative reversing and non-reversing components is required. Once the ideal modulation

parameters have been determined, the use of SSADSC for studying degradation may become more significant. Using a larger sample size may also improve the resolution of the non-reversing trace, allowing for further investigation of the relative degree of reversing to non-reversing melting in these systems.

Acknowledgements

This work was supported by NIH grant # 2R016M47636-05.

References

[1] Gangadharam P, Kailasam S, Srinivasan S, Wise DJ. Antimicrob Chemother 1994;33(2):265–71.
[2] Robertson D, Sivin I, Nash H, Braun J, Dinh J. Contraception 1983;27(5):483–95.
[3] Tornqvist N, Bjorklund L, Almqvist P, Wahlberg L, Stromberg I. Exp Neurol 2000;164(1):130–8.
[4] Siden R, Flowers W, Levy R. Biomaterials 1992;13(11):764–70.
[5] Wang C, Sengothi K, Lee TJ. Pharm Sci 1999;88(2):215–20.
[6] Rabowsky J, Dukes A, Lee D, Leong K. Ophthalmology 1996;103(5):800–7.
[7] Trope G, Cheng Y, Sheardown H, Liu G, Menon I, Heathcote J, Rootman D, Chiu W, Gould L. Can J Ophthalmol 1994;29(6):263–7.
[8] Yuan X, Dillehay L, Williams J, Williams J. Cancer Biother Radiopharm 1999;14(3):187–202.
[9] Wada R, Hyon S, Nakamura T, Ikada Y. Pharm Res 1991;8(10):1292–6.
[10] Nilsson C, Johansson E, Jackanicz T, Luukkainen T. Am J Obstet Gynecol 1975;122(1):90–5.
[11] Mathiowitz E, Kline D, Langer R. Scanning Microsc 1990;4(2):329–40.
[12] D'Souza M, DeSouza P. Drug Dev Ind Pharm 1998;24(9):841–52.
[13] Ogawara K, Yoshida M, Higaki K, Kimura T, Shiraishi K, Nishikawa M, Takakura Y, Hashida M. J Controlled Release 1999;59(1):15–22.
[14] Mumper R, Wang J, Klakamp S, Nitta H, Anwer K, Tagliaferri F, Rolland A. J Controlled Release 1998;52(1–2):191–203.
[15] Sanders LM, McRae GI, Vitale KM, Kell BA. J Controlled Release 1985;2:187–95.
[16] Langer R, Peppas N. J Macromol Sci, Rev Macromol Chem Phys 1983;c23:61–126.
[17] Teomim D, Fishbien I, Golomb G, Orloff L, Mayberg M, Domb A. J Controlled Release 1999;60(1):129–42.
[18] Park E, Maniar M, Shah J. J Controlled Release 1998;52(1–2):179–89.
[19] Carino G, Jacob J, Mathiowitz E. J Controlled Release 2000;65(1–2):261–9.
[20] Domb A, Israel Z, Elmalak O, Teomim D, Bentolila A. Pharm Res 1999;16(5):762–5.
[21] Hanes J, Chiba M, Langer R. Biomaterials 1998;19(1–3):163–72.
[22] Mathiowitz E, Kreitz M, Pekarek K. Macromolecules 1993;26(25):6749–55.
[23] Domb A, Mathiowitz E, Ron E, Giannos S, Langer R. J Polym Sci 1991;29:571.
[24] Mathiowitz E, Jacob J, Jong Y, Carino G, Chickering D, Chaturvedi P, Santos C, Vijayaraghavan K, Montgomery S, Bassett M, Morrell C. Nature 1997;386(6623):410–4.
[25] Huffman K, Casey D. J Polym Sci, Polym Chem Ed 1985;23:1939–54.
[26] Santos CA, Freedman BD, Leach KJ, Press DL, Scarpulla M, Mathiowitz E. J Controlled Release 1999;60(1):11–22.
[27] Mathiowitz E, Ron E, Mathiowitz G, Amero C, Langer R. Macromolecules 1990;23(13):3212.
[28] Modulated Temperature DSC from http://www.anasys.co.uk.
[29] Reading M. Trends Polym Sci 1993;1:248.
[30] Sichina B. PE instruments presentation 2000.
[31] Reading M, Hahn B, Crowe BS. US Patent 5,224,775, 1993.
[32] Reading M, Luget A, Wilson R. Thermochim Acta 1994;238:295.
[33] Boller A, Jin Y, Wunderlich B. J Therm Anal 1994;42:295.
[34] Wunderlich B, Jin Y, Boller A. Thermochim Acta 1994;238:277.
[35] Wunderlich, B. Course on Temperature Modulated Calorimetry, http://funnelweb.utcc.utk.edu/~athas/courses/tmdsc97.html, 1997.
[36] Sauer BB, Kampert WG, Neal Blanchard E, Threefoot SA, Hsiao SA. Polymer 2000;41:1099–108.
[37] Bailey, N. PhD Thesis. The University of Birmingham, Birmingham, 2000.